The Astrophysical Journal, 654:580–594, 2007 January 1

SPITZER 24 μm OBSERVATIONS OF OPEN CLUSTER IC 2391 AND DEBRIS DISK EVOLUTION OF FGK STARS

Nick Siegler,[1] James Muzerolle,[1] Erick T. Young,[1] George H. Rieke,[1] Eric E. Mamajek,[2] David E. Trilling,[1] Nadya Gorlova,[1] and Kate Y. L. Su[1]

Received 2006 July 10; accepted 2006 September 5

ABSTRACT

We present 24 μm *Spitzer* MIPS photometric observations of the $\sim$50 Myr open cluster IC 2391. Thirty-four cluster members ranging in spectral type from B3 to M5 were observed in the central square degree of the cluster. Excesses indicative of debris disks were discovered around one A star, six FGK stars, and possibly one M dwarf. For the cluster members observed to their photospheric limit, we find a debris disk frequency of 10^{+17}_{-3}% for B–A stars and 31^{+13}_{-9}% for FGK stars using a 15% relative excess threshold. Relative to a model of decaying excess frequency, the frequency of debris disks around A-type stars appears marginally low for the cluster's age while that of FGK stars appears consistent. Scenarios that may qualitatively explain this result are examined. We conclude that planetesimal activity in the terrestrial region of FGK stars is common in the first $\sim$50 Myr and decays on timescales of $\sim$100 Myr. Despite luminosity differences, debris disk evolution does not appear to depend strongly on stellar mass.

Subject headings: infrared: stars — open clusters and associations: individual (IC 2391) — planetary systems: protoplanetary disks

1. INTRODUCTION

Nearly all stars are believed to form with primordial accretion disks, but it is not clear whether the formation of planets is also a nearly universal process of stellar evolution. Answering this question would help us understand the incidence of planetary systems in the Galaxy. Current planet detection techniques, while continuously improving, all suffer from some instrument sensitivity limitation. Many of the planets may very well be insufficiently massive to be detected through gravitational recoil, too faint against the glare of the central star to be imaged directly, too small to significantly reduce the star's measured brightness, or positioned unfavorably along the line of sight to produce a lensing event.

Planetary debris disks, however, provide an additional approach. Debris disks contain micron-sized dust grains predominantly produced in collisions between larger sized bodies (such as rocks). These dust grains are heated by the parent star and reradiate at longer wavelengths. A key facet of debris disks is that the dust grains must be short-lived compared to the age of the system given the efficiency of typical loss mechanisms such as Poynting-Robertson drag and radiation pressure (with timescales of 10^6–10^7 yr). The dust must therefore be regenerated either through a continuous collisional cascade or through stochastic collisions. Therefore, the presence of dust implies the existence of larger bodies that can collide and produce dusty debris (Backman & Paresce 1993; Lagrange et al. 2000; Zuckerman 2001). The largest of these bodies could be meter-sized up to planet-sized, and we may well refer to them generally as planetesimals. *Therefore, any system with excess thermal emission implies planet formation at least to the extent of forming planetesimals*. The ability to measure thermal emission in the mid-infrared is therefore a powerful technique in identifying systems in which planetary system formation has occurred or is occurring. However, since debris disks are cool, optically and geometrically thin, and gas-poor, they are generally harder to detect than the primordial, optically thick accretion disks found around very young stars ($\lesssim$10 Myr).

The *Spitzer Space Telescope*'s unprecedented sensitivity in the mid-infrared allows for the first time a statistical study of debris disks and their evolution across a wide spectral range. Excesses detected at 24 μm generally imply temperatures on the order of 100 K. This equilibrium temperature is achieved in the vicinity of 1–5 AU for spectral types FGK and 5–30 AU for the more luminous B and A stars. By probing these distances in the mid-infrared, we are therefore studying potential planet-forming and planet-bearing regions around other stars. Building on earlier work from the *Infrared Astronomy Satellite* (*IRAS*) and *Infrared Space Observatory* (*ISO*) that showed that the amount of dust in debris disks steadily declines over time (e.g., Spangler et al. 2001; Habing et al. 2001), Rieke et al. (2005) showed that more than half of A-type stars younger than $\sim$30 Myr have mid-infrared excess. This result implies that planetary system formation occurs frequently around stars a few times more massive than the Sun. However, the same result also shows that up to $\sim$50% of the youngest stars have small or nonexistent excesses in the mid-infrared, pointing to a possible range of planetesimal formation and clearing timescales.

Can we expect similar behavior for lower mass, longer living, solar-like stars? Both *IRAS* and *ISO* were in general not sufficiently sensitive to detect the photospheric emission from lower mass stars. Only with *Spitzer* have mid-infrared surveys of lower mass stars begun (Gorlova et al. 2004, 2006; Young et al. 2004; Meyer et al. 2004; Stauffer et al. 2005; Kim et al. 2005; Beichman et al. 2005a; Chen et al. 2005, 2006; Bryden et al. 2006; Silverstone et al. 2006; Beichman et al. 2006). These studies conducted at 24 and/or 70 μm have shown that debris disks exist around solar-like stars at a wide range of possible distances ($\sim$1–50 AU) and temperatures ($\sim$10–650 K) with an age-dependent frequency. It is one of the goals of this investigation to constrain this age dependence. Continued surveys of stars with known ages at mid-infrared wavelengths will bring us nearer to understanding how debris disks evolve and ultimately will provide constraints on planet formation timescales.

[1] Steward Observatory, University of Arizona, Tucson, AZ; nsiegler@as.arizona.edu.
[2] Harvard-Smithsonian Center for Astrophysics, Cambridge, MA.

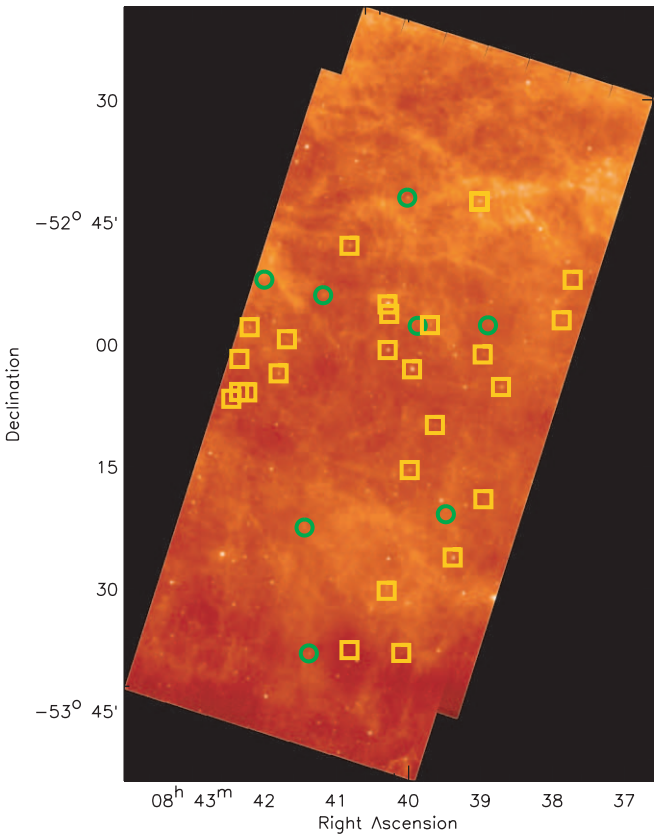

FIG. 1.—A 0.97 deg^2 mosaic of the central region of IC 2391 taken with the MIPS 24 μm channel. *Open circles*: Debris disk candidates. *Open squares*: Cluster members with no apparent 24 μm excess. The point-source FWHM is 5.7″ and the plate scale is 1.25″ pixel^{-1}. The image is displayed with a linear stretch and epoch J2000.0 celestial coordinates.

In this investigation we use the 24 μm channel on *Spitzer* to study the incidence of debris disks in the open cluster IC 2391. IC 2391 is estimated to be 50 $\pm$ 5 Myr old (Barrado y Navascués et al. 2004), an age consistent with both theoretical (Chambers 2001) and observational (Kleine et al. 2002) timescales of terrestrial planet formation. It is believed to be of intermediate size with $\sim$100–200 members. At a distance of 154 pc (Forbes et al. 2001), the cluster is among the closest and best studied. Furthermore, its proximity allows for the detection of photospheric emission at mid-infrared wavelengths from low-mass stars. With little observed 24 μm cirrus structure and visible extinction [$E(B-V) = 0.006 \pm 0.005$; Patten & Simon 1996], IC 2391 offers an attractive combination of age, distance, and background in which to study debris disks.

The aim of this investigation is to measure the incidence of debris disks found around $\sim$50 Myr stars across a broad range of spectral types. We discuss the ensemble properties of excesses in IC 2391 by placing our data in context with other relevant samples. In the process we begin characterizing the evolution of debris disks around FGK stars, and compare this result to that previously established for more massive A stars.

2. OBSERVATIONS AND DATA REDUCTION

The Multiband Imaging Photometer for *Spitzer* (MIPS; Rieke et al. 2004) was used to image a 0.97 deg^2 area (0.66° $\times$ 1.47°) centered on IC 2391 (R.A. = 08^{h}40^{m}16.8^s, decl. = −53°06′18.9″; J2000.0) on 2004 April 9. The 24 μm observations used the medium scan mode with half-array cross-scan offsets resulting in a total exposure time per pixel of 80 s. The images were processed using the MIPS instrument team Data Analysis Tool (Gordon et al. 2005), which calibrates the data, corrects distortions, and rejects cosmic rays during the co-adding and mosaicking of individual frames. A column-dependent median subtraction routine was applied to remove any residual patterns from the individual images before combining them into the final 24 μm mosaic.

While MIPS in scan-mode provides simultaneous data from detectors at 24, 70, and 160 μm, this study is based on only the 24 μm channel. The longer wavelength channels are insensitive to stellar photospheric emissions at the distance of IC 2391, and in addition no cluster stars were detected at 70 or 160 μm.

We measured the 24 μm flux density of individual sources in a 15″ aperture using the standard PSF-fitting photometry routine `allstar` in the IRAF data reduction package DAOPHOT. We then applied an aperture correction of 1.73 to account for the flux density outside the aperture, as determined from the STinyTim 24 μm PSF model (C. W. Engelbracht et al. 2007, in preparation). Finally, fluxes were converted into magnitudes referenced to the Vega spectrum using a zero point for the [24] magnitude of 7.3 Jy (from the MIPS Data Handbook, ver. 2.3). Typical 1 σ measurement uncertainties for the MIPS 24 μm fluxes are 50 μJy plus $\sim$5% uncertainty in the absolute calibration (C. W. Engelbracht et al. 2007, in preparation). The two are independent of each other and dominated by the latter.

The 24 μm mosaic of the central region of IC 2391 is displayed in Figure 1. It likely covers a bit less than half of the spatial extent of the entire cluster (Barrado y Navascués et al. 2001). There is relatively little background cirrus or extended emission in the field of view. As explained in § 3.3, MIPS is sensitive to detecting the photospheres of mid-K dwarfs at the distance of IC 2391.

3. RESULTS AND ANALYSIS

3.1. *IC 2391 Cluster Members Detected at* 24 μm

To determine the fraction of $\sim$50 Myr stars possessing 24 μm emission excess, we must match the detected sources in our mosaic to bona fide IC 2391 cluster members. There are 1393 sources detected at 24 μm in the *Spitzer* MIPS mosaic (Fig. 1) with a limiting magnitude of 11.7 mag (0.15 mJy). Using a 2″ search radius, 505 of these sources matched objects in the 2MASS All-Sky Point Source Catalog (Cutri et al. 2003), providing both corresponding near-infrared photometry and standardized 2MASS celestial coordinates. It is expected that all IC 2391 cluster members detected at 24 μm in the MIPS mosaic will have corresponding 2MASS detections since the faintest known cluster members in the literature have $K_s \approx 14.5$ mag (M5–M7; Barrado y Navascués et al. 2004) (2MASS K_s sensitivity limit is $\simeq$15.3 mag).

To obtain V-band magnitudes and proper motions for cluster member selection, we ran the list of 505 sources through the United States Naval Observatory Flagstaff Station (USNOFS) image and catalog archive database NOMAD (Naval Observatory Merged Astrometric Dataset;[3] Zacharias et al. 2004a). This database selects for each source the "best" astrometric and photometric data chosen from its catalogs[4] and merges the results into a single data set. Due to the cluster's distance, most of the sources had measured USNO-B1.0 (Monet et al. 2003) or UCAC2 (Zacharias et al. 2004b) proper motions. In the cases where V magnitudes were not available through the database, we used alternate catalogs through the VizieR

[3] See http://www.nofs.navy.mil/data/fchpix.

[4] For catalog details and references see http://www.nofs.navy.mil/nomad/nomad_readme.html.

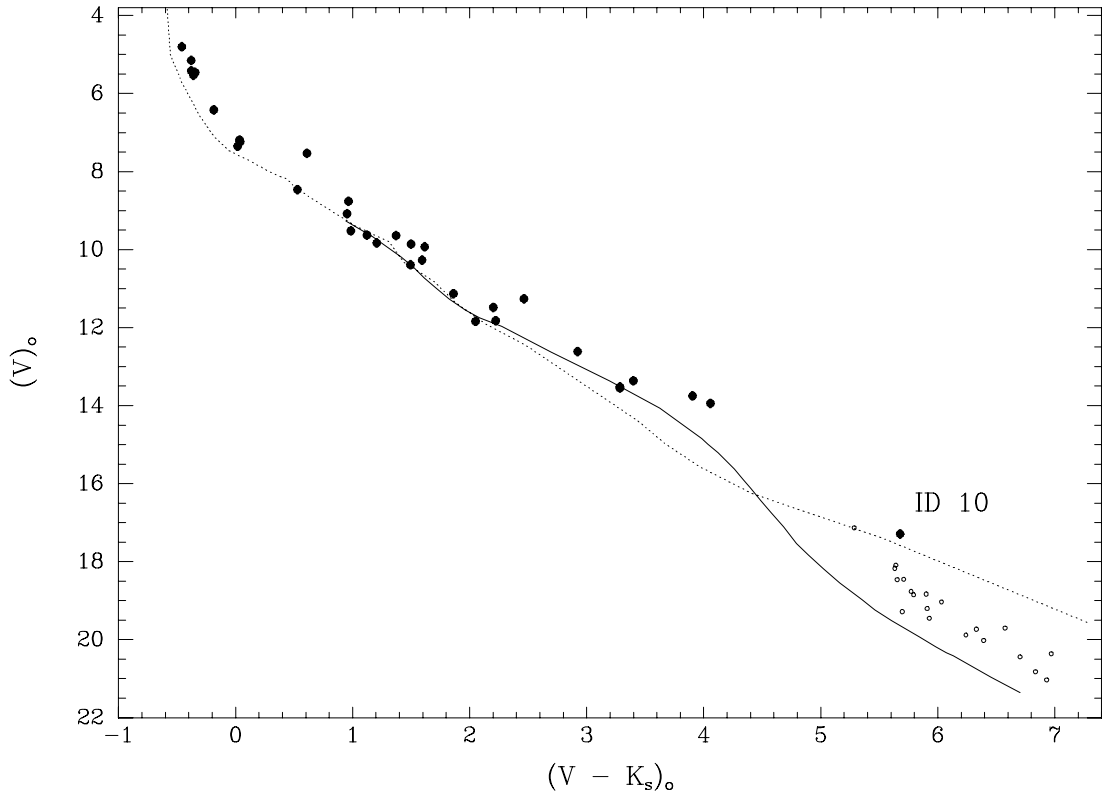

FIG. 2.—Dereddened V vs. $V - K_s$ CMD of 33 IC 2391 cluster members (*filled circles*) observed in our 24 μm mosaic (Fig. 1); stars have been uniformly dereddened using $E(B - V) = 0.006$ (Patten & Simon 1996) and the near-infrared reddening laws of Cambrésy et al. (2002). Not included is the brightest star of the cluster *o* Velorum (ID 20), which is saturated at K_s. Overplotted are 50 Myr theoretical isochrones from Siess et al. (2000) (*dotted line*) and Baraffe et al. (1998) (*solid line*) placed at the distance of IC 2391. Since the models begin diverging at $V - K_s \gtrsim 4.4$, we also plot 22 M4–M7 dwarfs (*small open circles*) that are spectroscopically confirmed cluster members from Barrado y Navascués et al. (2004) to illustrate the empirical sequence for the coolest known members. The M5 dwarf ID 10, the faintest member in our sample detected at 24 μm, appears consistent with membership but as a likely binary.

Search Service or photometry directly from literature sources listed hereafter.

To our list of 505 stars with *V, J, H,* K_s, and [24] photometry, we applied the following membership criteria in sequential order (numbers in parenthesis indicate the number of sources that still remained after the criterion was applied):

1. object positions located on the stellar main sequence locus of a dereddened $J - H$ versus $H - K_s$ color-color diagram that indicate membership (228);
2. object positions located on dereddened V versus $V - K_s$ (Fig. 2) and K_s versus $J - K_s$ color-magnitude diagrams (CMDs) that indicate membership (111);
3. proper motions within 2 σ of the cluster mean (≈95% of true members; estimated through a χ^2 comparison to the mean *Hipparcos* cluster motion,[5] which includes the object's proper-motion uncertainty and an assumed intrinsic velocity dispersion of 1 mas yr^{-1}, where 1 mas yr^{-1} ≈ 0.7 km s^{-1}; Bevington & Robinson 1992, p. 71); using this criterion is expected to result in only ≈5% of bona fide cluster members being rejected (26).

The evolutionary models of Baraffe et al. (1998) and Siess et al. (2000) were used to determine the mean cluster CMD isochrones and color-color positions for 50 Myr old stars placed at the distance of IC 2391 (154 pc). We selected candidate members using a band 1 mag in apparent magnitude on either side of the mean theoretical isochrones and 0.1 mag in color-color positions. The selection bands are sufficiently broad to take into account photometric, distance, age, binarity, and model uncertainties; reddening is not a factor here. However, with the cluster being close to the Galactic plane ($b = -6.90$), there is no clear separation between the field stars and the location of the cluster isochrones. We reduce the interloper contamination of our sample by using the combination of photometric and kinematic measurements as listed above. For later type stars, however, the evolutionary models appear to diverge at $V - K_s \gtrsim 4.4$, and hence we used the spectroscopically confirmed mid-M dwarfs from Barrado y Navascués et al. (2004) to define an empirical cluster sequence for later type members.

Only those sources that satisfied all of the criteria were classified as members and are included in the statistics. From the original 505 sources, 26 met all three criteria for membership. As a consistency and completeness check, we compare our list to probable cluster members from the literature lying in the MIPS field of view in Figure 1. While there have been many cluster membership investigations of IC 2391 measuring proper motions, optical and near-infrared photometry, radial velocities, rotational velocities, X-ray emission, spectral classification, and spectral youth diagnostics, there is no single complete listing. The Open Cluster Database[6] as provided by C. F. Prosser and J. R. Stauffer is composed of both members and candidate members extracted from the literature up until 1997. Later cluster membership references come from Simon & Patten (1998), Patten & Pavlovsky (1999), Barrado y Navascués et al. (2001), Forbes et al. (2001), Randich

[5] Mean *Hipparcos* cluster motion is $\mu_\alpha \cos\delta = -25.06 \pm 0.25$ mas yr^{-1}, $\mu_\delta = 22.7 \pm 0.22$ mas yr^{-1} (Robichon et al. 1999).

[6] See http://www.noao.edu/noao/staff/cprosser.

TABLE 1
General Characteristics of IC 2391 Cluster Members with 24 μm Detections

ID Number	R.A. (J2000.0)	Decl. (J2000.0)	Spectral Type	V (mag)	$V - K_s$ (mag)	$v \sin i$ (km s^{-1})	Binarity?[a]	$\log(L_X/L_{bol})$	Common Names[b]
1	8 37 47.0	−52 52 12.4	F5	9.65	1.14	...	No	...	HD 73777
2	8 37 55.6	−52 57 11.0	G9	11.50	2.22	...	No?	−3.70	VXR 02a
3	8 38 44.8	−53 05 25.4	B8	6.44	−0.17	...	Yes	−5.99	HD 73952, VXR 04
4	8 38 55.7	−52 57 51.7	G2	10.29	1.61	34	No	−4.47	SHJM 1, VXR 05
5	8 38 58.8	−53 19 12.7	M3	13.77	3.92	<7	SB2	−3.38	VXR 06a
6	8 38 59.9	−53 01 26.3	F5	9.66	1.39	21.0	No	−3.98	VXR 07
7	8 39 02.8	−52 42 38.4	K:	11.28	2.48[c]	...	Yes	...	HD 74009B
8	8 39 03.4	−52 42 39.7	F3	8.78	0.98	...	Yes	−3.80[d]	HD 74009A, VXR 08
9	8 39 23.9	−53 26 23.0	B5	5.44	−0.36	...	No	...	HD 74071
10[e]	8 39 29.6	−53 21 04.4	M5	17.31	5.69	...	Yes?	...	PP 07
11	8 39 38.8	−53 10 07.2	G:	9.95	1.63	...	No	−3.68	VXR 11, CD −52 2482
12	8 39 43.0	−52 57 51.1	F2	9.10	0.97	...	No	<−5.14	HD 74117
13	8 39 53.0	−52 57 56.9	K0	11.86	2.07	16	No	−3.63	SHJM 6, VXR 12
14	8 39 57.6	−53 03 17.0	B5 IV	5.17	−0.36	...	SB	<−7.28	HD 74146
15	8 39 59.4	−53 15 39.4	A1p	7.21	0.05	...	SB	−4.90	HD 74169, VXR 13
16	8 40 01.6	−52 42 12.6	A7	8.48	0.55	...	No	<−5.75	HD 74145
17	8 40 06.2	−53 38 06.9	G0	10.41	1.51	47	No	−3.59	VXR 14
18	8 40 16.2	−52 56 29.2	G9	11.84	2.24	22.0	No	−3.25	VXR 16a
19	8 40 17.5	−53 00 55.4	B7	5.55	−0.34	...	SB	<−6.95	HD 74196
20[f]	8 40 17.6	−52 55 19.0	B3 IV	3.59	−0.55[f]	...	No	...	o Velorum, HD 74195
21	8 40 18.3	−53 30 28.8	K4	13.54	3.30	8	No	−3.28	VXR 18a
22	8 40 48.5	−52 48 07.1	A0	7.26	0.05	...	SB	−4.92	HD 74275, VXR 21
23	8 40 49.1	−53 37 45.4	G1	11.15	1.88	...	No	−3.27	VXR 22a
24	8 41 10.0	−52 54 10.6	F6	9.85	1.22	43	SB1?	−4.48	HD 74340, VXR 30
25	8 41 22.8	−53 38 09.2	F3	9.54	1.00	...	No	...	HD 74374
26	8 41 25.9	−53 22 41.6	K3e	12.63	2.94	90	SB?	−3.00	SHJM 3, VXR 35a
27	8 41 39.7	−52 59 34.1	K7.5	13.38	3.42	18	Yes?	−3.32	SHJM 8, VXR 38a
28	8 41 46.6	−53 03 44.9	A3	7.55	0.63	...	No	-	HD 74438
29	8 41 57.8	−52 52 14.0	K7.5	13.57	3.30	<15	No	−3.21	SHJM 9, VXR 41
30	8 42 10.0	−52 58 03.9	A1	7.37	0.03	...	No	<−6.69	HD 74516
31	8 42 12.3	−53 06 03.8	F5	9.88	1.52	67:	No	−3.95	VXR 44
32	8 42 18.6	−53 01 56.9	M2e	13.96	4.07	95	Yes	−3.41	SHJM 10, VXR 47
33	8 42 19.0	−53 06 00.3	B9p	5.48	−0.33	...	Yes?	−6.67	HD 74535
34	8 42 25.4	−53 06 50.2	B3 IV	4.82	−0.44	...	SB	−7.79	HD 74560, VXR 48

Notes.—Units of right ascension are hours, minutes, and seconds, and units of declination are degrees, arcminutes, and arcseconds. Celestial coordinates are from 2MASS.

[a] SB: Spectroscopic binary; SB1: single-line spectroscopic binary; SB2: double-line spectroscopic binary.

[b] VXR: Patten & Simon (1996); SHJM: Stauffer et al. (1989); PP: Patten & Pavlovsky (1999).

[c] $(K_s)_{2MASS}$ derived from $(K_s)_{Denis}$ and $(J - K_s)_{Denis}$ using the Carpenter (2001) transformation relation.

[d] X-ray measurements from Patten & Simon (1996) include emission from both IDs 7 and 8.

[e] Li abundance potentially inconsistent with membership; see discussion in § 3.6.

[f] The reported 2MASS K_s photometry is flagged due to saturation. We do not include this source in any of the figures using K_s, nor is it included in the excess frequency calculations due to its early spectral type.

et al. (2001), and Barrado y Navascués et al. (2004). All 26 sources from our analysis were also classified in the literature as probable or possible cluster members, with all but two (IDs 7 and 11) having spectral confirmation. Having satisfied our membership criteria, we are confident that these 26 sources are bona fide IC 2391 cluster members, and we list them in Tables 1 and 2.

In addition, there were seven sources that were originally deselected due to proper motions slightly exceeding our χ^2 criterion or not measured but are cited as probable cluster members in the literature. All seven—IDs 8, 10, 13, 21, 27, 29, and 32—have photometry consistent with membership according to our first two criteria. ID 8 (HD 74009) is an F3 star whose proper motion we recalculated using additional catalog points and now satisfies the third criterion. Using an 88 yr baseline, we also verified that ID 8 is part of a 5.5″ binary whose companion, ID 7, is also detected in our 24 μm image. The companion independently satisfies the first two membership criteria, but with large V-band uncertainty. We thus add ID 7 in addition to the original 26 sources. ID 10 (PP 07; Patten & Pavlovsky 1999) is an M5 dwarf that we discuss in more detail in § 3.6. ID 13 (SHJM 6 = VXR PSPC 12), ID 27 (SHJM 8 = VXR PSPC 38a = VXR 17), and ID 29 (SHJM 9 = VXR 41) (Stauffer et al. 1989; Patten & Simon 1996) all have evidence of youth through strong Li I detections (λ6707; Randich et al. 2001). ID 32 (SHJM 10 = VXR 47; Stauffer et al. 1989; Patten & Simon 1996) is observed to be an M2e dwarf with a radial velocity within 1 σ of the cluster mean (Stauffer et al. 1997), Li abundance (Randich et al. 2001), and colors consistent with an early-M dwarf. However, its position on a CMD requires it to be a near-equal-mass multiple system. Lastly, ID 21 (VXR PSPC 18a) has no measured proper motion but is X-ray active (Patten & Simon 1996) and has youth signatures (Randich et al. 2001) and a radial velocity consistent with cluster membership (Stauffer et al. 1997). Thus we add these eight sources to raise our final sample size to 34 objects and include them in Tables 1 and 2.

Spectral types in Table 1 were obtained from the references previously mentioned or from SIMBAD; rotational velocities were

TABLE 2
INFRARED PROPERTIES OF IC 2391 CLUSTER MEMBERS WITH 24 μm DETECTIONS

ID Number	$K_s - [24]$ (mag)	[24] (mag)	σ([24]) (mag)	24 μm Flux (mag)	Excess Ratio[a] (mag)	24 μm Excess?	70 μm Flux[b] (mJy)
1	−0.06	8.57	0.03	2.71	0.94	No	<63
2	0.37	8.91	0.04	1.98	1.34	No	<82
3	−0.11	6.72	0.03	14.90	0.93	No	<108
4	0.25	8.43	0.03	3.09	1.23	Yes	<88
5	0.14	9.71	0.04	0.95	0.86	No	<102
6	0.07	8.20	0.03	3.83	1.05	No	<100
7	−0.03[c]	8.83	0.04	2.14	0.93	No	<71
8	0.05	7.75	0.03	5.81	1.04	No	<52
9	−0.20	6.00	0.03	28.98	0.86	No	<73
10	1.10	10.52	0.06	0.45	1.63	Yes	<52
11	0.07	8.25	0.03	3.67	1.04	No	<73
12	0.14	7.99	0.03	4.65	1.13	No	<52
13	0.22	9.58	0.04	1.08	1.18	Yes	<148
14	−0.18	5.71	0.03	37.92	0.88	No	<109
15	−0.08	7.24	0.03	9.28	0.95	No	<94
16	0.61	7.32	0.03	8.59	1.77	Yes	<159
17	0.07	8.83	0.03	2.14	1.04	No	<75
18	0.06	9.54	0.04	1.12	1.01	No	<74
19	−0.14	6.03	0.03	28.27	0.91	No	<54
20[d]	−0.08[d]	4.22	0.03	149.05	0.97	No	<136
21	0.12	10.12	0.05	0.65	0.99	No	...
22	−0.10	7.31	0.03	8.70	0.93	No	<102
23	0.03	9.25	0.03	1.46	0.99	No	...
24	0.43	8.20	0.03	3.84	1.47	Yes	<124
25	0.75	7.79	0.03	5.58	1.98	Yes	...
26	0.26	9.44	0.04	1.23	1.18	Yes	<115
27	0.22	9.74	0.04	0.93	1.07	No	<93
28	−0.05	6.97	0.03	11.84	0.96	No	<67
29	0.35	9.92	0.05	0.79	1.22	Yes	...
30	−0.11	7.44	0.03	7.70	0.93	No	...
31	0.03	8.34	0.03	3.37	1.00	No	<68
32	0.30	9.59	0.04	1.07	0.96	No	...
33	−0.10	5.91	0.03	31.57	0.94	No	...
34	−0.20	5.47	0.03	47.48	0.87	No	...

[a] Ratio of observed 24 μm flux density to the predicted photospheric flux density at 24 μm.
[b] Upper limits; the 24 and 70 μm mosaics cover slightly different areas of the sky and hence some 24 μm detections do not have 70 μm upper limit measurements.
[c] $(K_s)_{2MASS}$ derived from $(K_s)_{Denis}$ and $(J - K_s)_{Denis}$ using the Carpenter (2001) transformation relation.
[d] The reported 2MASS K_s photometry is flagged due to saturation. We do not include this source in any of the figures using K_s.

obtained from Stauffer et al. (1989, 1997), and fractional X-ray luminosities [$\log(L_X/L_{bol})$] were obtained from Patten & Simon (1996). For completeness, we list in Appendix A three objects that are classified in the literature as cluster members but through this study are shown to be unassociated. None of these sources had 24 μm excess.

3.2. *Determining* 24 μm *Photospheric Colors*

Our goal is to measure the fraction of IC 2391 cluster members possessing evidence of debris disks by measuring 24 μm flux densities in excess of their expected photospheric emission. We now establish a photospheric baseline emission using a $V - K_s$ versus $K_s - [24]$ color-color diagram to help identify these excess sources across a broad range of spectral types.

When the sources are all of similar distance and spectral type, a K_s versus $K_s - [24]$ CMD can identify potential excesses empirically (see Fig. 3 in a Pleiades disk study by Stauffer et al. 2005). Even without knowing the exact photospheric color at 24 μm, Stauffer et al. (2005), in consideration of their uncertainties and relative excesses, designate stars with $K_s - [24] \gtrsim 0.1$ as candidate debris disk sources. However, for a broader range in photospheric temperature (color), results from Gautier et al. (2006) show that the $K_s - [24]$ photospheric color gradually reddens with cooler effective temperatures until abruptly turning redward for spectral types later than M0. We also see evidence of this behavior in a larger disk survey of the Pleiades conducted by Gorlova et al. (2006).

The $V - K_s$ color is a good proxy for spectral type. The two bands are sufficiently separated in wavelength space to trace temperatures/spectral types, as well as to break degeneracies that beset near-infrared colors near the K-M spectral type transition. The $K_s - [24]$ color is a very good diagnostic for mid-infrared excess since for stars earlier than M dwarfs, it is only weakly dependent on stellar temperature with both bands in the Rayleigh-Jeans regime. Using the $K_s - [24]$ as a mid-infrared excess diagnostic, however, requires the K_s band to be photospheric. Near-infrared excess is a diagnostic for optically thick primordial disks probing emission from active accretion at radii $\lesssim 0.1$ AU. We find no evidence for near-infrared excesses from $H - K_s$ colors in our sample. Furthermore, for stars older than 10 Myr, the innermost regions of primordial disks have largely dissipated (Haisch et al. 2001).

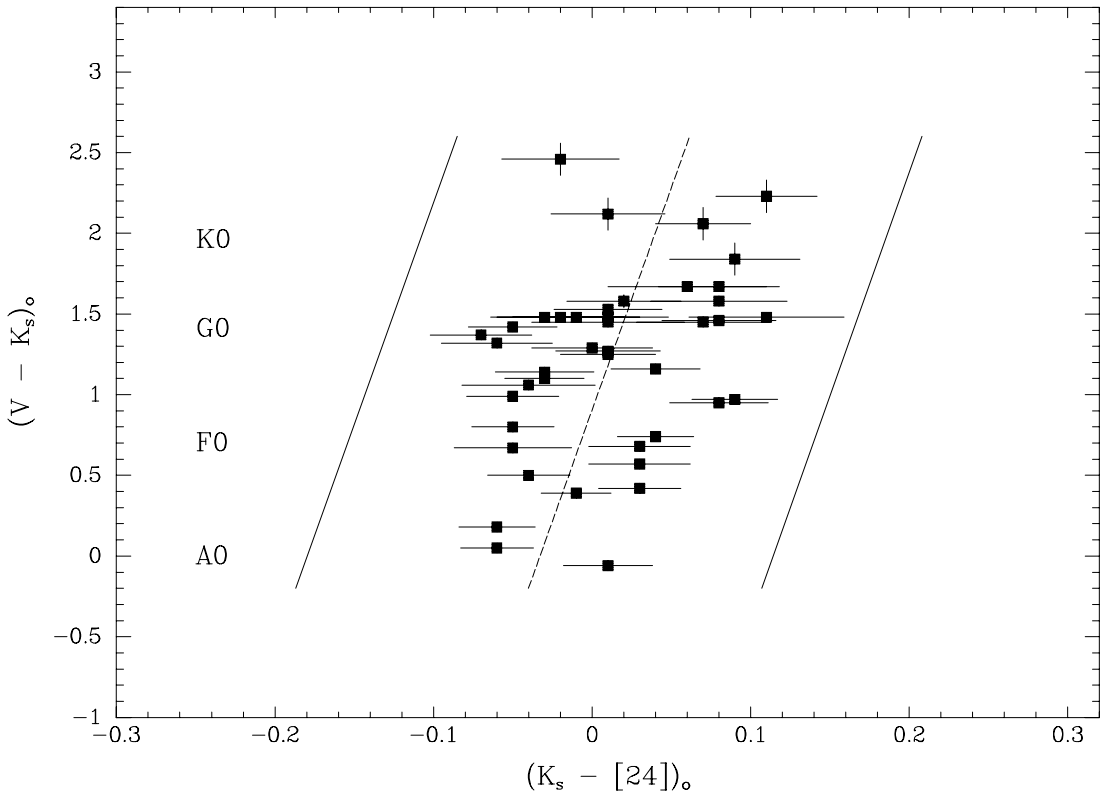

FIG. 3.—Dereddened $V - K_s$ vs. $K_s - [24]$ color-color diagram plotting 57 late-B to mid-K cluster members (*filled squares*) of the Pleiades open cluster possessing no apparent 24 μm excess (Stauffer et al. 2005; Gorlova et al. 2006). The linear fit to the data (*middle dashed line*) with a 3 σ scatter of 0.15 mag (*outer solid lines*) for stars with colors between $0.05 \leq V - K_s \leq 3.0$ is described in Gorlova et al. (2006). We interpret the region within the 3 σ outer solid lines as the empirical photospheric locus for late-B to mid-K stars.

Thus we conclude cluster member emission at K_s is photospheric and that significant $K_s - [24]$ deviations from photospheric values imply the presence of a circumstellar component.

The lack of a large sample of cluster members with no apparent 24 μm excess in IC 2391 across a wide spectral type range makes establishing a pure empirical photospheric locus potentially inaccurate. There are only 16 apparently nonexcess stars with $V - K_s \lesssim 3.0$. On the other hand, a mid-infrared investigation of the Pleiades by Gorlova et al. (2006) offers a large homogeneous 24 μm stellar sample with metallicity and distance similar to those of IC 2391, with only slightly older age. Gorlova et al. (2006) have identified 57 Pleiades members with good quality detections at K_s and 24 μm and no evidence of mid-infrared excess. We plot these 57 stars with colors $0.05 \leq V - K_s \leq 3.0$ in Figure 3 to illustrate the relative tightness of the distribution. The age difference between IC 2391 and the Pleiades will have negligible effect on the intrinsic $K_s - [24]$ color with both wavelengths on the Rayleigh-Jeans side of the emission spectrum for the range of stars in which we are interested. The effect on the $V - K_s$ color is less than 0.1 mag according to a comparison of Siess et al. (2000) tracks. This is not surprising as pre–main-sequence stars at 50 Myr are already quite close to the main sequence. As we use the $K_s - [24]$ color as the primary diagnostic for mid-infrared excess, a 10% variation in $V - K_s$ or less will have very little effect on identifying excesses when using Figure 3. Hence, for the $K_s - [24] \sim 0$ regime ($0.05 \leq V - K_s \leq 3.0$), we use the larger sample of Pleiades members with no apparent mid-infrared excess to construct an empirical photospheric locus of stars on a $V - K_s$ versus $K_s - [24]$ color-color diagram. This photospheric locus is applicable for spectral types from late-B to mid-K stars.

To establish the photospheric locus for M dwarfs, we rely on the field M-dwarf survey of Gautier et al. (2006). We plot their points (*small open circles*) with matching *V*-band magnitudes in Figure 4. The photospheric colors indeed turn redward with increased slope for stars with $V - K_s \gtrsim 3.6$. We compare this locus with the predicted $V - K_s$ colors for 50 Myr stars (Siess et al. 2000) with the spectral type/$K_s - [24]$ relation from Gautier et al. (2006) (*dashed line*).

3.3. *Sources with Apparent* 24 μm *Excess*

Since the precision of the 24 μm photometry in the Pleiades data set is very similar to ours, we adopt the Pleiades 3 σ relative excess threshold ($\sigma = 0.05$ mag) as the criterion for thermal excess in our IC 2391 study. A cluster member whose 24 μm flux density exceeds its predicted photospheric emission at this wavelength by at least 15% is a debris disk candidate. We refer to the ratio of observed to predicted flux density as the 24 μm excess ratio and will discuss its evolution for FGK stars in § 4.3. We apply in Figure 4 this photospheric locus for A–K stars along with the empirical photospheric locus for M dwarfs to our IC 2391 sample. We uniformly deredden the stars using $E(B - V) = 0.006$ and the IR reddening laws described in Cambrésy et al. (2002) (assuming $A_{[24]} \sim 0$).

In the $V - K_s \leq 3.0$ regime in Figure 4, we identify seven debris disk candidates: IDs 2, 4, 13, 16, 24, 25, and 26. Of the three detected cluster M dwarfs, we observed only one obvious excess: the M5 dwarf ID 10 (discussed further in § 3.6). For the color regime not fitted by our models ($3.0 < V - K_s < 3.6$), we assume in Figure 4 a simple diagonal fit connecting the upper and lower regimes. This is consistent with the positions of late-type stars

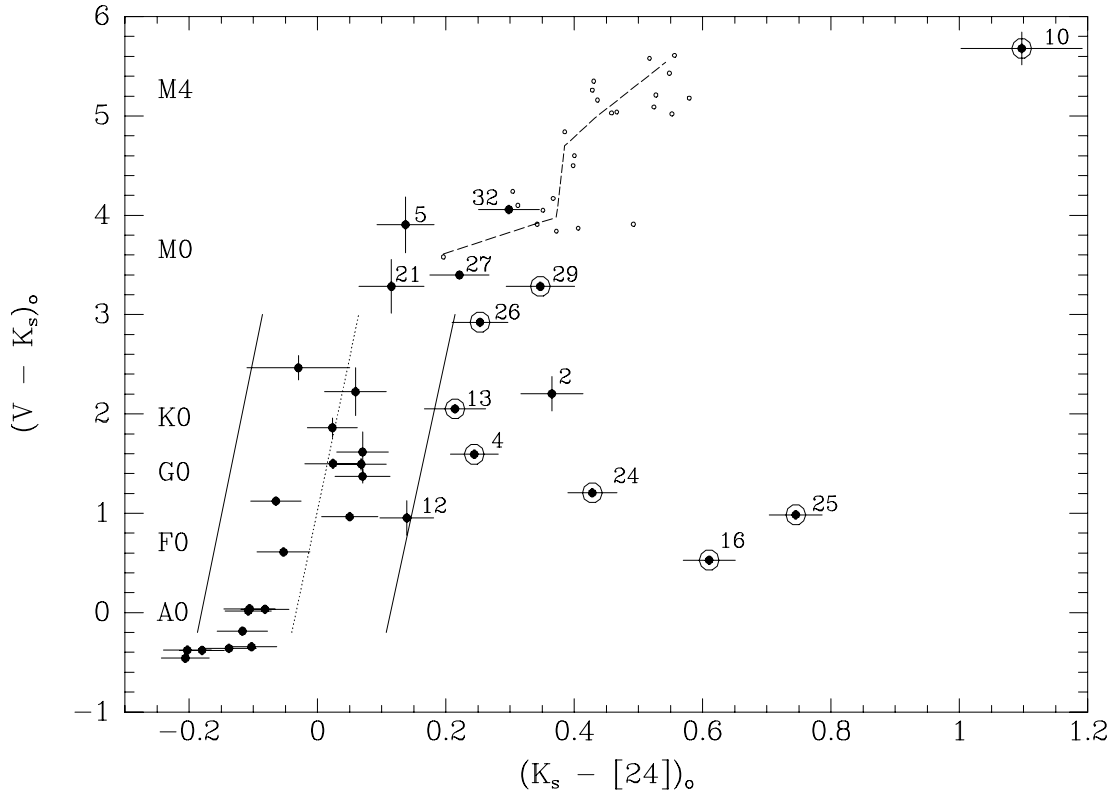

FIG. 4.—Dereddened $V - K_s$ vs. $K_s - [24]$ color-color diagram plotting 31 members (*filled circles*) of the IC 2391 open cluster. The brightest star in the cluster, B3 IV *o* Velorum (ID 20), is omitted due to saturated K_s photometry. The dereddened Pleiades photospheric locus with its mean (*dotted line*) and 3 σ scatter (*solid lines*) from Fig. 3 is overplotted. Sources redder than the 3 σ Pleiades relative excess threshold possess $K_s - [24]$ flux ratios in excess of expected photospheric colors and are considered to be debris disk candidates (*large open circles*). To estimate the photospheric locus for stars with $V - K_s$ colors redder than the Pleiades locus ($V - K_s > 3.0$), we plot field M dwarfs (*small open circles*) from a 24 and 70 μm investigation by Gautier et al. (2006). We also plot the theoretical photospheric $V - K_s$ colors of 50 Myr stars (Siess et al. 2000) matched to a spectral type/$K_s - [24]$ relation from the Gautier et al. M dwarf sample (*dashed line)*. Both profiles, along with a few members from IC 2391, show a redward turn for photospheres of late-type stars near $V - K_s \sim 3.0$. ID numbers of some of the cluster members are shown. The mid-infrared excess of ID 2 may be associated with a background giant (see § 3.4).

ID 5, 21, and 27 and results in one more candidate excess source, ID 29.

The images of the nine stars initially identified as debris disk candidates were visually inspected at 24 μm to ensure they match a point-spread function and do not include potential contamination by heated cirrus or background sources. In addition, the stars were analyzed in the higher resolution, near-infrared 2MASS images[7] for elongation due to possible tight binaries. Only source ID 2 (VXR 02a, G9; Patten & Simon 1996) showed elongation in the 24 μm image, due to a faint source appearing 6.6″ away. Patten & Simon (1996) classify this faint companion object as a K3 V, but its near-infrared colors and position on the cluster CMD are more consistent with a background K giant and hence it is possible that the 24 μm excess may be due to dust from an evolving background giant and not the cluster member ID 2. Therefore, we do not classify ID 2 as a debris disk candidate.

In total, we identify eight cluster members with evidence of debris disks: one A star, six FGK stars, and one M dwarf. We circle the eight in Figures 1 and 4 and indicate them as 24 μm excess objects in Table 2.

The candidate debris disks presented here are the first observed in IC 2391. A report of possible 25 μm *IRAS* excesses around several of the cluster A and early-F stars (Backman et al. 1991) is not confirmed. Six members (all B stars) have 12 μm *IRAS* detections, all of which are photospheric. None have *IRAS* detections at wavelengths ≥ 60 μm. In addition, none of the members have been previously detected with ISO. We summarize the overall number and frequency of excess objects by spectral type in Table 3 and discuss their interpretation in § 4.

The excess frequency of a sample is defined as the ratio of the number of excess sources to the total number of sources. We include in this ratio only those IC 2391 cluster members whose photospheres are detectable at 24 μm. We define this minimum flux density sensitivity as the completeness limit of our sample, calculated at the turnover in the K_s brightness distribution of all the sources in our MIPS image with 24 μm detection ($K_s < 9.9$). This brightness corresponds to spectral type ~K4 in IC 2391. Detections fainter than the completeness limit may be biased toward excesses.

While we identify 34 cluster members in our mosaic, eight are removed from our statistical analysis. Four have K_s magnitudes fainter than our photospheric completeness level (IDs 10, 21, 27, 29), and another two are binaries whose individual components are outside the completeness limit (IDs 5 and 32). The last two, IDs 20 and 34, are both B3 IV stars. It is known that early B stars are sufficiently hot to emit free-free emission that can also contribute 24 μm flux (Chokshi & Cohen 1987). Hence, using a 15% threshold, we report an overall excess frequency for the cluster of $0.23^{+0.10}_{-0.06}$ (6/26; excess frequency uncertainties are reported throughout this report as 1 σ binomial probability distributions; see Appendix in Burgasser et al. 2003).

While there were no detections of IC 2391 cluster members with the MIPS 70 μm channel, we calculate upper flux limits at the 24 μm source positions using aperture photometry with a

[7] See http://irsa.ipac.caltech.edu/applications/2MASS/IM/.

TABLE 3
FRACTION OF IC 2391 CLUSTER MEMBERS WITH 24 μm EXCESS

Spectral Type	Number of Members in This Sample	Number of Excess Stars[a]	Excess Frequency[b]
B	7	0	$\sim$0.0 (0/5)[c]
A	5	1	$0.20^{+0.25}_{-0.08}$ (1/5)
FGK	19	6	$0.31^{+0.13}_{-0.09}$ (5/16)
M[d]	3	1	...
B5–A9 (A type)	10	1	$0.10^{+0.17}_{-0.03}$ (1/10)
F5–K4 (solar type)	13	4	$0.31^{+0.14}_{-0.10}$ (4/13)

[a] Excesses defined as sources with $K_s - [24]$ colors lying on or redward of the 3 σ Pleiades photospheric baseline shown in Fig. 4. The 24 μm excess fluxes are $\geq$15% above the mean photospheric flux as a function of spectral type.
[b] Ratio of the number of excess stars to the total number of stars in a spectral bin. All sources included in the excess frequency have 24 μm sensitivity to the photospheric flux (spectral type $<$ K4).
[c] Spectral types $<$B5 are removed from the excess frequency statistics due to possible free-free emission contamination.
[d] All three systems are most likely binaries with integrated brightness sufficiently large to be detected at 24 μm; one, however, has a very strong 24 μm excess. None of the 24 μm detections are sensitive to photospheric emission.

1.83 pixel radius aperture and 1.927 aperture correction (STinyTim 70 μm PSF model; K. Gordon et al. 2007, in preparation). The 70 μm upper limits are listed in Table 2.

3.4. *Contamination*

With a relatively flat background and little cirrus emission, the most likely contaminant in IC 2391 is confusion from random line-of-sight positional overlap with distant, optically faint but infrared-bright galaxies and AGNs, showing no sign of elongation in the MIPS image. What is the probability of such an accurate chance alignment? For example, with $\sim$2000 extragalactic sources per square degree at 0.5 mJy (Papovich et al. 2004), a flux less than our completeness limit but greater than our detection limit, the probability of a chance background source observed within 0.5″ of a cluster member is 0.4% ($\pi[(0.5'')^2/(0.97 \times 60^2)] \times 2000 \times 32$). Except for ID 10 and ID 29, the faintest excess sources, the remaining excess candidates are at least a factor of 2 brighter and the extragalactic contamination is significantly lower.

In addition, we looked for positional offsets between our 24 μm excess sources and the corresponding 2MASS positions that could potentially indicate fake excess emission from a superimposed object. The average offset between all our MIPS objects and 2MASS positions for members from Table 1 is 0.6″. Except for ID 29, which is the second faintest excess candidate in the sample (and not included in our frequency statistics), the sources fall within a 1″ circle centered on the 0.6″ systematic offset on a $\Delta\alpha$ versus $\Delta\delta$ plane.

3.5. *Debris Disk Correlations with Other Stellar Properties*

Due to both its age and proximity, IC 2391 has been the subject of several rotational velocity and X-ray studies (Stauffer et al. 1989, 1997; Patten & Simon 1993, 1996; Simon & Patten 1998; Marino et al. 2005). To assess correlations between cluster members with and without evidence for debris disks with other stellar parameters, we matched the cluster members in Table 1 with information regarding binarity, rotation ($v \sin i$), and X-ray luminosity [$\log (L_X/L_{bol})$] from the literature. As also observed by Stauffer et al. (2005) and Gorlova et al. (2006) in their investigations of the Pleiades, we find no clear correlations between 24 μm excess sources and any of these stellar properties.

3.6. *An Interesting Possible Cluster Member: PP 7*

ID 10 (PP 7; Patten & Pavlovsky 1999) is a spectroscopically measured M5 dwarf (Barrado y Navascués et al. 2004) with an observed 24 μm flux density approximately 1.6 times the predicted photospheric level. PP 7 is the faintest star in Table 1 to have a 24 μm detection *and* have an excess; however, it is 3 times above the MIPS 24 μm detection limit. Its positions in both near-infrared and optical CMDs (Fig. 2), as well as in the near-infrared color-color diagram, are consistent with membership, but only as a nearly equal-mass binary system. The Na I doublet (λ8200) equivalent width and Hα emission line are consistent with a young, late M dwarf. Using five astrometric positions we have calculated its proper motion to be $\mu_\alpha \cos\delta = -45.0 \pm 10.1$ mas yr^{-1}, $\mu_\delta = 20.8 \pm 10.7$ mas yr^{-1}. Compared to IC 2391's mean motion (Robichon et al. 1999), PP 7 gives a kinematic χ^2 of 3.9 for 2 degrees of freedom (i.e., 14% of bona fide cluster members should have proper-motion values more deviant). Hence, PP 7 appears to be kinematically consistent with membership in IC 2391.

PP 7 appears to possess, however, a Li abundance anomaly. Barrado y Navascués et al. (2004) report a weak Li measurement (S/N $\sim$ 3) in its spectrum despite the star being about 2 mag brighter than the empirical Li depletion boundary for the cluster at K_s. The possibility, as mentioned above, that the star may be an equal-mass binary brings it 0.75 mag closer to the cluster Li depletion boundary. While there exists the possibility that PP 7 is a very young, nearby star but unassociated with IC 2391, the simpler hypothesis may be that it is a cluster member whose Li has simply not burned as fast as other members of similar mass. A radial velocity measurement would most likely confirm membership. If proven to be a member, it would be only the fourth M dwarf older than 10 Myr known to have a mid-infrared or submillimeter excess (AU Mic, GJ 182, 2MASS J08093547−4913033; Song et al. 2002; Liu et al. 2004; Young et al. 2004).

4. DISK FREQUENCY OF IC 2391 AND IMPLICATIONS FOR DEBRIS DISK EVOLUTION

We find eight IC 2391 cluster members with spectral types between A and M possessing 24 μm excess consistent with debris disks. There are two interesting aspects to our results: (1) a possible dearth of 24 μm excess around A-type stars, and (2) an abundance of 24 μm excess around FGK stars. We now discuss these results, put them in the context of stars in clusters of similar and different ages, and interpret the implications for debris disk evolution.

4.1. *Dearth of Debris Disks around Early-Type Stars in IC 2391?*

Because of their high temperatures and luminosities, A stars are very efficient at illuminating the dust in debris disks, yet they are not so hot, as are early-B stars, that they excite gaseous disks that might masquerade as debris dust. Consequently, debris systems around A-type stars (B5–A9) have been studied particularly

TABLE 4
24 μm Excess Frequencies of A-Type Stars from *Spitzer* MIPS Surveys

Name	Excess Frequency	Age (Myr)	Sample Size	Excess Frequency References
Upper Cen Lupus.....	$0.44^{+0.12}_{-0.11}$	16 ± 2	16	1
NGC 2547.....	$0.44^{+0.12}_{-0.10}$	30 ± 5	18	2, 3
IC 2391	$0.10^{+0.17}_{-0.03}$	50 ± 5	10	4
M47.....	$0.32^{+0.10}_{-0.12}$	80 ± 20	31	5
Pleiades	$0.25^{+0.12}_{-0.07}$	115 ± 20	20	6
NGC 2516.....	$0.25^{+0.07}_{-0.05}$	150 ± 20	51	5
Hyades.....	$0.09^{+0.16}_{-0.03}$	625 ± 50	11	1

Note.—A-type stars are defined here as stars with spectral type B5–A9; earlier B stars are omitted to minimize the possibility of 24 μm detection from gaseous disk free-free emission rather than from warm dust in a debris disk.

References.—(1) Su et al. 2006; (2) Young et al. 2004; (3) N. Gorlova et al. 2007, in preparation; (4) this paper; (5) Rieke et al. 2005; (6) Gorlova et al. 2006.

thoroughly. The largest surveys of this nature are Rieke et al. (2005) (266 stars) and Su et al. (2006) (160 stars), who used both *Spitzer* and *IRAS* observations to study debris disk frequencies and evolution. Their samples, composed of both cluster members and field objects, range in age between 5 and 850 Myr, and all the observations at 24–25 μm are sensitive to photospheric levels.

How does the debris disk frequency of A-type stars in IC 2391 compare to the larger surveys? To create a single robust sample to which we could compare our results, we combined the two samples of Rieke et al. and Su et al., removed the *IRAS* sources (which have larger scatter than the *Spitzer* data), used a common relative excess threshold criterion ($\geq$15%), and only considered sources with estimated ages $\geq$10 Myr. Whenever there was source duplication we used the more recent Su et al. 24 μm excess ratio results due to improved reduction procedures and fitting to theoretical photosphere models. The combined data set consists of 276 stars, which we place in arbitrary age bins. For the 31–89 Myr age bin, the excess frequency is $0.44^{+0.12}_{-0.10}$ (8/18). Thus, nearly half of the stars between 31 and 89 Myr have evidence of debris disks. For the same B5–A9 spectral type range in IC 2391, we find an excess frequency of $0.10^{+0.17}_{-0.03}$ (1/10). If we use the binomial distribution where the probability of "success" is $0.44^{+0.12}_{-0.10}$, the probability that these two results are drawn from the same distribution is about 3%.

There are three possibilities to explain this result: (1) it may be just a statistical deviation, given the only moderate probability that the difference is significant; (2) it may signal that the simple smooth decay with age used to characterize debris disks as demonstrated by Rieke et al. (2005) is an oversimplification; or (3) it might indicate that the cluster environment has influenced the debris disk evolution. The first possibility cannot be ruled out without observations of additional clusters at similar ages. Nevertheless, the latter two are worth exploring because it is of interest to see whether variations in the debris disk frequencies in clusters might be possible and what their causes might be.

How does this frequency compare to clusters of other ages? In Table 4 we list the excess frequencies from *Spitzer* 24 μm surveys of A-type stars from open clusters (and an OB association) with sample sizes $\geq$10 and plot them in Figure 5. In each cluster, the same relative excess threshold of 15% above the predicted photospheric emission has been used. Age estimates and their uncertainties are obtained from references within those listed in Table 4.

The seven open clusters and the association closely follow the larger combined field and cluster sample. This is not unexpected with only the Pleiades and IC 2391 not already included in the larger combined sample. While the fraction of stars with debris disks for the other clusters matches the overall behavior of the entire sample, IC 2391's disk frequency appears disproportionately low. Since its behavior does not seem to be reflected in the other cluster results, it does not represent an overall departure from the smooth decline in activity. That is, there is no evidence in favor of our second hypothesis.

We now consider the third possibility, that the cluster environment might be responsible. Unlike the marginally smaller fraction of measured excesses found among the A-type stars in IC 2391, Figure 4 shows that excesses around the FGK stars appear to be more common. Is there a physical scenario that can explain the behavior of *both* stellar types?

Metallicity is not a likely issue in this case because IC 2391 has a metallicity (Fe/H $= -0.03 \pm 0.07$; Randich et al. 2001) comparable to that of other clusters with higher frequencies of A-type excesses (i.e., the Pleiades and M47; Nissen 1988; Randich et al. 2001). In addition, a dependence of the incidence of excesses on metallicity has not been seen in solar analogs (Greaves et al. 2006).

A hypothesis invoking mass segregation whereby the most massive stars settle toward the cluster center where stellar densities, and hence disk interactions, are highest does manage to explain why less-massive stars would have higher disk frequencies. However, theoretical simulations of the effects of primordial disk interactions in clusters the size of IC 2391 ($\sim$100–200 members) during the early period of gas dissipation predict low interaction rates (Adams et al. 2006). In addition, this phenomenon is not observed in other open clusters that should already have experienced mass segregation (such as the Pleiades and the Hyades).

Interestingly, Sagar & Bhatt (1989), conducting a kinematic survey of proper-motion data for eight clusters with ages ranging from 8 to 300 Myr, found IC 2391 to be the *only* cluster that showed mass dependence as a function of intrinsic proper motion dispersions. The higher mass stars in IC 2391 were measured to have lower velocity dispersions than the lower mass stars, suggesting mass segregation. Their results, however, suffer from several observational uncertainties, including low proper-motion accuracies and incomplete IC 2391 cluster membership. Nevertheless, their claim is intriguing.

Another possibility centers on the photoevaporation of primordial disks. This process may be greatly accelerated around very luminous O stars (e.g., Hollenbach et al. 2000). The formation of such a star in a cluster is subject to small-number statistics (Elmegreen 2004), and it is possible that some clusters would have subjected their members' primordial disks to this effect, while others would not. Given the short lifetimes of O stars, the direct traces of the

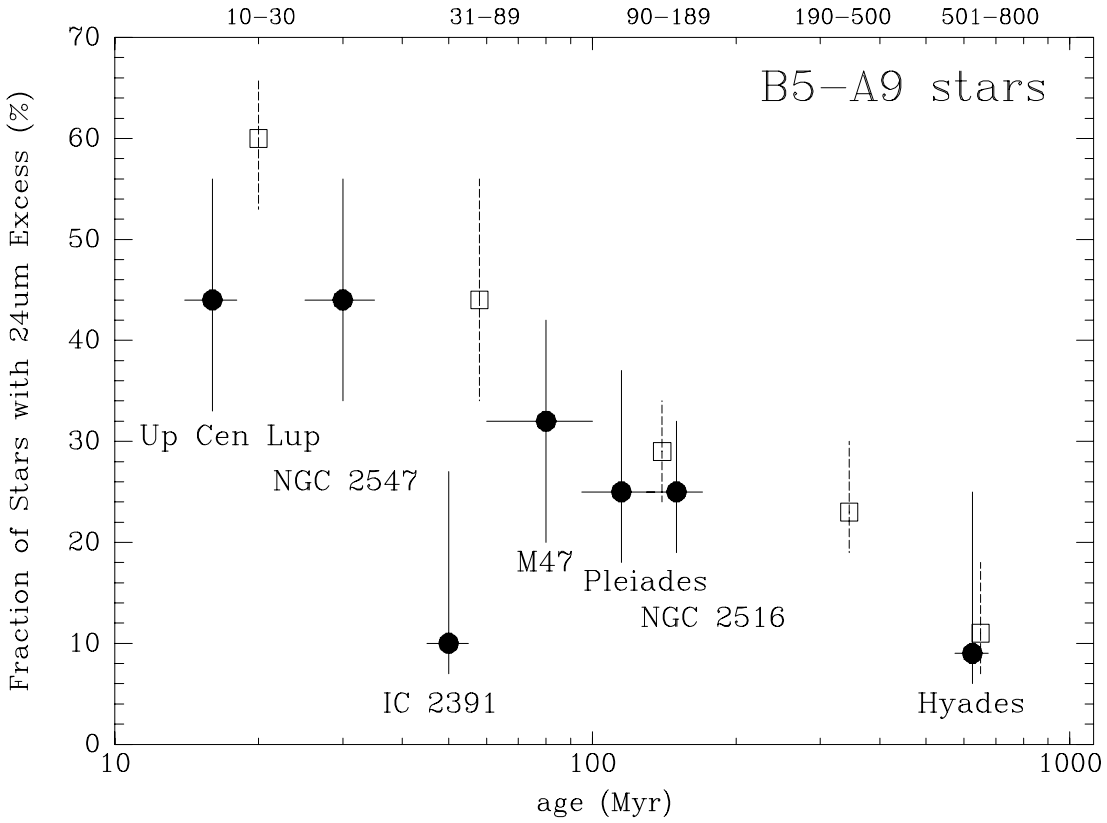

FIG. 5.—Frequency of A-type stars (B5–A9) with 24 μm excess as a function of age. Plotted as filled circles are the excess frequencies from *Spitzer* MIPS observed open clusters and a stellar association (data and references listed in Table 4). Also shown in open squares are mean 24 μm excess frequencies from age bins (listed across the top of the figure) from the combined MIPS-only surveys of Rieke et al. (2005) and Su et al. (2006). Error bars are 1 σ binomial distribution uncertainties, and age uncertainties are taken from the cluster references in Table 4. In all cases a 15% relative excess threshold was used. Note that the IC 2391 excess frequency appears comparatively low for its age.

star would have disappeared by the age of IC 2391. To account for the differences between the A-type and FGK stars in this cluster, however, requires either that mass segregation play a key role on timescales short enough to expose the A-type stars and their primordial disks to the UV radiation of O stars *before* significant planetesimal formation, or that photoevaporation be less efficient inward (toward the star), at radii where G stars radiate at 24 μm ($\sim$5 AU). Theoretical models differ on whether photoevaporation could behave in this manner (Johnstone et al. 1998; Richling & Yorke 1998; Matsuyama et al. 2003; Throop & Bally 2005). Although relaxation timescales in clusters of the size of IC 2391 are short enough ($\sim$1 Myr; Binney & Tremaine 1987, p. 190) to support this hypothesis, the high primordial disk frequency of $\sim$40% in NGC 2244 ($\sim$2 Myr), despite its including many O stars (Z. Balog et al. 2007, in preparation), would argue against it.

In summary, although it would be interesting to search for some of the effects we have discussed in other clusters, none of them gives a solid explanation for the behavior of IC 2391. For the present, we need to assume that the lack of A-type star debris systems may just be due to statistics.

4.2. *Abundance of Debris Disks around Solar-Type Stars in IC 2391*

Seven cluster members in IC 2391 with spectral types F–M show evidence of 24 μm excess. Considering just the spectral types within the completeness limit (<K4) and a 24 μm relative excess threshold of 15%, the excess frequency of FGK stars is $0.31^{+0.13}_{-0.09}$ (5/16). In fact, even around solar-type stars (F5–K7), the excess frequency is $\sim$0.31 (4/13). Debris disks around solar-type stars in IC 2391 appear to be common.

Unlike the A-star surveys of Rieke et al. (2005) and Su et al. (2006), there is to date no comprehensive mid-infrared study in the literature of the fraction of solar-type stars with debris disks over a broad range of ages. We list the excess frequencies for known *Spitzer* 24 μm surveys sensitive to photospheric emissions of F, G, and possibly K stars in open clusters (and an OB association) in Table 5. Depending on distance or target sample, the spectral type corresponding to the 24 μm completeness limit brightness varies in each cluster. We state any assumptions made in estimating the debris disk frequency of each cluster in Appendix B.

The evolution of the excess frequency of FGK stars is shown in Figure 6. The IC 2391 results fill an age gap in the previous studies between 30 and 100 Myr. The relatively large 24 μm excess frequency observed around FGK stars in IC 2391 ($\sim$31%) appears consistent for its age with an evolutionary decay model. There are two important results here: (1) the IC 2391 result implies that planetesimals around solar-type stars are *still* undergoing frequent collisions in terrestrial planet-forming regions at $\sim$50 Myr, and (2) the fraction of FGK stars with 24 μm excess appears to decay similarly to the trend seen for A-type stars.

While the uncertainties in the excess frequencies of the youngest systems are considerable, Figure 6 clearly illustrates that planetesimal activity (collisions) within the terrestrial planet zones of FGK stars ($\sim$1–5 AU) is common during at least the first 50 Myr. This is consistent with the epoch of terrestrial planet formation in our own solar system (Kleine et al. 2002; Jacobsen 2005). In fact,

TABLE 5
24 μm Excess Frequencies of FGK Stars from *Spitzer* MIPS Surveys

Name	Excess Frequency	Spectral Type Range	Age (Myr)	Sample Size	Excess Frequency References
Sco Cen[a]	$0.40^{+0.25}_{-0.08}$	G	16 ± 2	35	1
NGC 2547.....	$0.33^{+0.12}_{-0.08}$	F	30 ± 5	21	2
IC 2391	$0.31^{+0.13}_{-0.09}$	F–K4	50 ± 5	16	3
Pleiades	$0.09^{+0.06}_{-0.02}$	F–K6	115 ± 20	53	4, 5
Hyades.....	0.00 + 0.03	G	625 ± 50	51	6
Field stars.....	0.03 ± 0.02	F5–K5	4000[b]	69	7

[a] Includes only stars from the subgroups Upper Centaurus Lupus and Lower Centaurus Crux.
[b] Median age of the sample.
References.—(1) Chen et al. 2005; (2) N. Gorlova et al. 2007, in preparation; (3) this paper; (4) Stauffer et al. 2005; (5) Gorlova et al. 2006; (6) based on preliminary information from Cieza et al. 2005, a conference poster (see Appendix B for additional comments); (7) Bryden et al. 2006.

planetesimal systems around FGK stars continue being collisionally active even within the first few hundred million years. Several hundred million years later, however, mid-infrared excesses in the ~1–5 AU regions become rare. A survey of 69 nearby, solar-like field stars with median age ~4 Gyr found only two with 24 μm excess meeting or exceeding the 15% relative excess threshold (Bryden et al. 2006). Also, the evolutionary decays presented in Figure 6 are only aggregate behaviors; even at ages $\gtrsim$500 Myr large episodic excesses, while quite rare, do appear (e.g., Beichman et al. 2005b). The rarity of large impacts in mature systems is consistent with both the models of Kenyon & Bromley (2004a) and the cratering record of the terrestrial planets (Strom et al. 2005; Gomes et al. 2005). We illustrate this further in § 4.3.

Combining with the results of Gorlova et al. (2006) the debris disk frequency around FGK stars follows an excess decay behavior similar to that of the more massive A-type stars. Despite the overall similarity of behavior, one could also conclude from Figure 6 that the FGK decay characteristic timescale appears shorter than that of the A-type stars. This is possibly, however, a luminosity effect rather than a mass-dependent effect (since the more luminous A stars heat up larger annuli of dust to the levels detectable at 24 μm). Until longer wavelength observations can probe larger

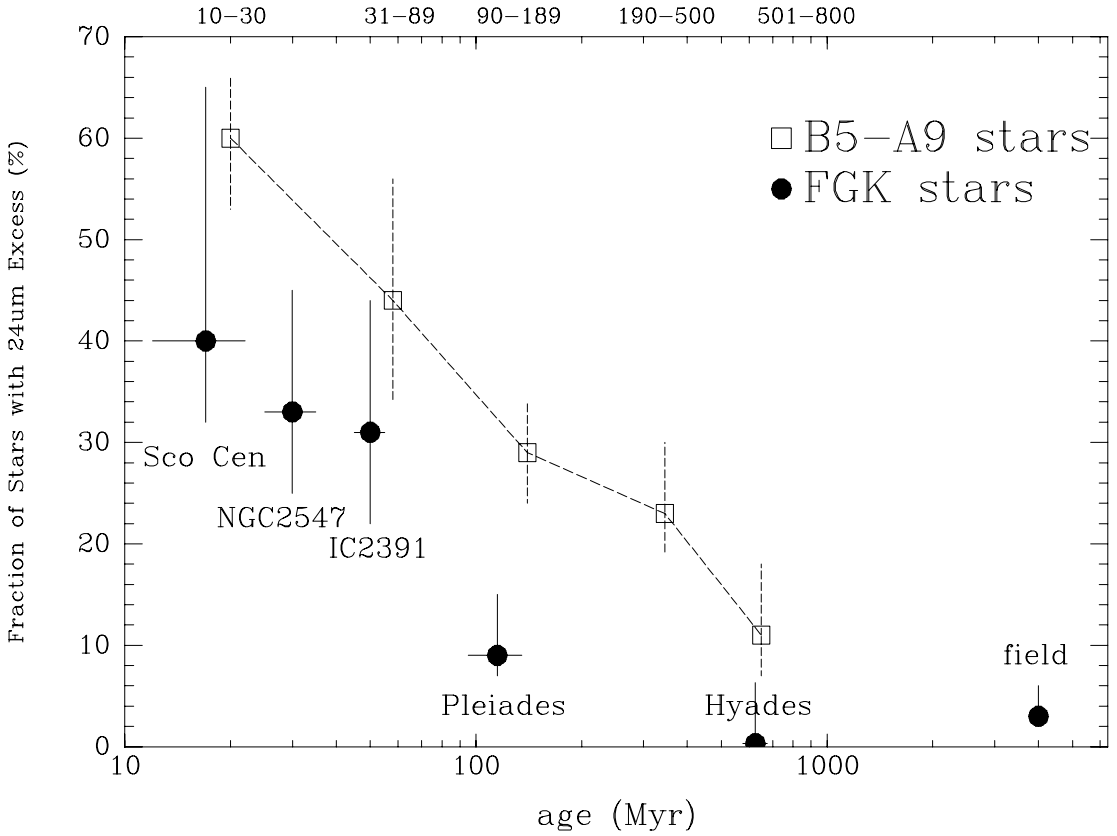

Fig. 6.—Fraction of stars with spectral types F, G, and/or K with 24 μm excess as a function of age. Plotted as filled circles are the excess frequencies of these stars from *Spitzer* MIPS observed clusters and an association (references given in Table 5; additional comments are made in Appendix B). As a comparison, we also plot the mean 24 μm excess frequencies of A-type stars (*open boxes*) from the combined MIPS-only data of Rieke et al. (2005) and Su et al. (2006) as shown in Fig. 5 (we connect the A-type points with a dashed line to help distinguish the two populations). In all cases, a 15% relative excess threshold was used. Vertical error bars are 1 σ binomial distribution uncertainties, and age uncertainties are taken from the cluster references listed in Table 5. Despite probing different annular regions, the decline in the excess frequency of the FGK stars suggests a decline in the collision rate between planetesimals with stellar age similar to that of the more massive A-type stars.

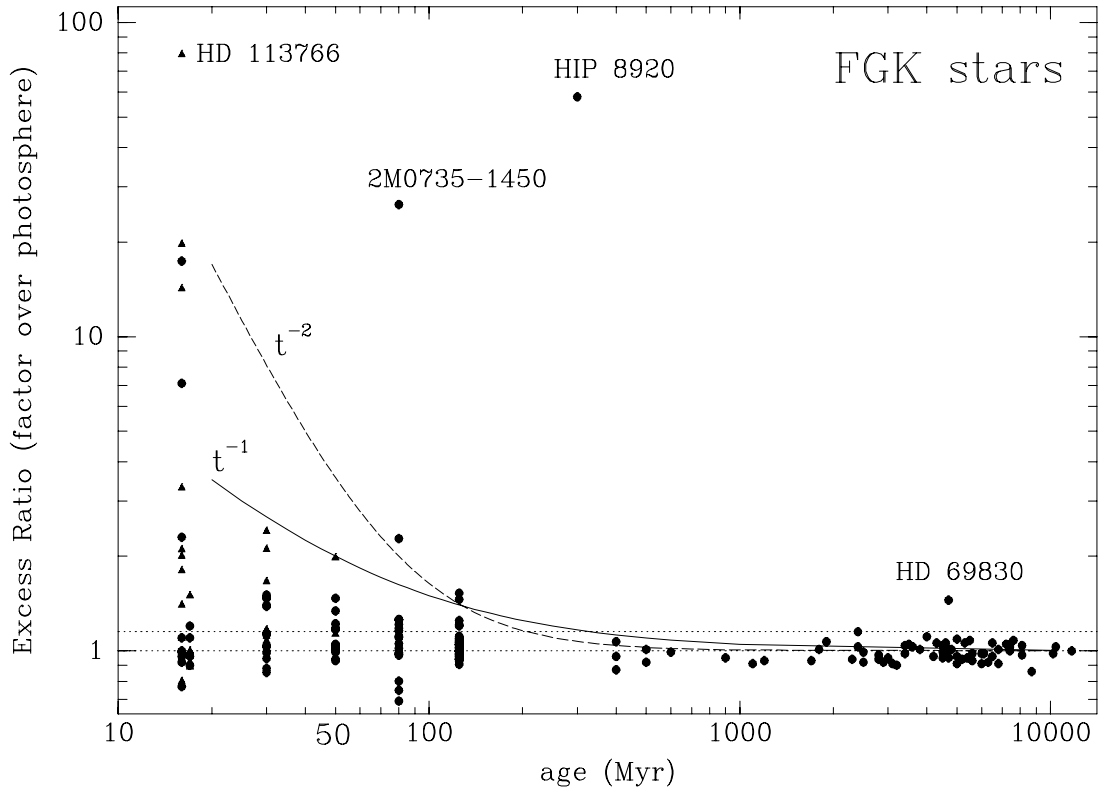

FIG. 7.—The 24 μm excess ratio vs. age for FGK stars. The excess ratio is the measured flux density to that expected from the stellar photosphere alone; a value of 1 represents no excess (*lower horizontal dotted line*). The upper horizontal dotted line represents the 1.15 relative excess threshold used in this study. F0–F4 stars are shown as filled triangles, while F5–K7 stars ("solar-like") appear as filled circles. The solid curve is an inverse time dependence, and the dashed curve is inverse time-squared. All of the points have been observed with *Spitzer* at 24 μm and, with a few noted exceptions, are part of the disk investigations listed in Table 5. Additions are M47 data (Gorlova et al. 2004), the 30 Myr HD 12039 (Hines et al. 2006), and the 300 Myr HIP 8920 (Song et al. 2005). Omitted from this figure is HD 152404 from Upper Centaurus Lupus (~17 Myr, F5 V; Chen et al. 2005) with a reported excess ratio of 202. The size of the excess coupled with its age suggests the possibility that the large excess may be due to a long-lived primordial disk. IC 2391's data are shown above its labeled age of 50 Myr.

distances around FGK stars for evidence of cooler dust, we conclude from Figure 6 that *debris disk evolution does not appear to be strongly dependent on stellar mass*.

Infrared excesses may originate from cascading collisions among asteroid-sized objects. However, some systems may be in a quiescent phase and not currently exhibit infrared excesses. In others, a wave of planet formation may have already passed through the regions probed at 24 μm (~1–5 AU), and planetesimal collisions may be occurring undetected at larger distances (Kenyon & Bromley 2004b). This implies that the debris disk incidence reported here actually gives a lower limit to the fraction of stars possessing planetesimals or undergoing planetesimal formation. Since a third of the stars have significant planetesimal-collision-generated excess emission at ~50 Myr, and the incidence of debris disks possibly rises at earlier ages, *it is likely that planetesimals form around the majority of solar-like stars*. However, even a more intriguing conclusion can be drawn if planetesimal collisions must be driven by gravitational perturbations from planet-sized objects, in which case it may be true *that most primordial disks around solar-like stars evolve to form planetary systems*.

4.3. *The Evolution of* 24 μm *Excesses around FGK Stars*

Understanding how the 24 μm excess evolves over time around FGK stars may provide insights to the collision history in the terrestrial planet region. Taking luminosity differences into account, we now explore the evolution of the excess ratio, which we defined in § 3.3. The 24 μm excess ratios of FGK stars in our IC 2391 sample range between 0.9 and 2.0, with a median of 1.1. In Figure 7 we plot these results, along with the excess ratios of FGK stars from the other clusters listed in Table 5, as a function of time. We also add two known solar-type stars not members of clusters but with measured mid-infrared excesses: HIP 8920 (300 Myr, G0 V; Song et al. 2005) and HD 12039 (30 Myr, G3–5; Hines et al. 2006). The upper envelope of the excess ratios appears to decrease rapidly within the first ~25 Myr, followed by a gentler decay with characteristic timescale of ~100 Myr. This early rapid decay may represent the final clearing of disks that are transitional between the primordial and debris stages. By several hundred million years, the mean 24 μm flux is close to photospheric.

Overplotted onto Figure 7 are an inverse time (*solid line*) and an inverse time-squared (*dashed line*) decay. While more data at younger ages would better define the fit, the inverse time decay appears to best match the data's upper envelope at ages $\gtrsim$20 Myr. Larger inverse powers overestimate the number of large excesses observed at earlier times. An inverse time decay is qualitatively consistent with collisions being the dominant grain destruction mechanism (Dominik & Decin 2003). Chen et al. (2006) show that for a main-sequence F5 star with dust mass between 0.001 and 1 $M_\oplus$, the collision lifetimes for average-sized grains is *always* shorter than the Poynting-Robertson and corpuscular wind drag lifetimes at radial distances <100 AU. Dominik & Decin (2003) and Wyatt (2005) conclude that all observed debris disks are in the collision-dominated regime.

The evolution of the observed excess ratios shown in Figure 7 may be best interpreted as the evolution of dust generation from planetesimal collisions around FGK stars. As planetesimals

are gravitationally scattered out of planetary systems, grow into Moon-sized objects or larger, or are ground down and removed via Poynting-Robertson drag, their fewer numbers result in less frequent but occasionally powerful collisions, producing copious amounts of dust. Observationally, this translates to a decreasing mean 24 μm flux excess ratio with occasional large outliers, as shown in Figure 7. Potential examples of stars with excess appearing as spikes indicating that such collisions have occurred recently (in the past ~million years) in their planetary systems are 2M 0735−1450 (80 Myr, F9; Gorlova et al. 2004) HIP 8920 (300 Myr, G0 V; Song et al. 2005), and HD 69830 (2 Gyr, K0; Beichman et al. 2005b).

Based on the rarity of objects with evidence of recent collisions and the generally low incidence of 24 μm excess, we draw a conclusion similar to that of Rieke et al. (2005): *large collisions occur after the initial period of terrestrial planet formation as episodic, stochastic events*. The general decay in the excess ratio may very well correspond to the decline of the collision frequency within the inner parts of a planetary system analogous to the asteroid belt of our own solar system. The larger excess ratios observed at earlier periods may be very reminiscent of our understanding of events in the early solar system, in which an early period ($\lesssim$100 Myr) of frequent and catastrophic collisions (e.g., the birth of the Moon) was followed by a declining rate of planetesimal impacts, followed by one last brief period of heavy bombardment of ~600–700 Myr (Strom et al. 2005; Gomes et al. 2005).

The general behavior of the FGK stars in Figure 7 is remarkably similar to the corresponding figure for A stars (Rieke et al. 2005). Besides the inverse time decay of the excess ratio and episodic outliers at ages older than about a hundred million years, Figure 7 also illustrates another similarity between the two populations: the fraction of stars that have no or little 24 μm excess at a given age. This phenomenon occurs even for the youngest FGK stars despite their overall higher probability of having mid-infrared excesses. Analogous to the previous conclusion from A-type star studies (Spangler et al. 2001; Decin et al. 2003; Rieke et al. 2005), this possibly points to a distribution of planet formation and clearing timescales even within young stellar clusters. Given the uniform behavior, the range of 24 μm excess measured over time should eventually provide quantitative constraints for theoretical models of planetary system evolution.

The results from numerical simulations investigating the evolution of dust generation from planetesimal collisions around solar-type stars by Kenyon & Bromley (2005) show a qualitative similarity to the observed behavior in Figure 7. Kenyon & Bromley (see their Fig. 4) show both a steady decline of the 24 μm excess ratio after ~1 Myr due to the depletion of colliding bodies and episodic large increases due to individual massive collisions. However, there are a number of observed behaviors where the simulations do not yet match. The characteristic timescales of the simulations appear shorter than what is observed. For example, at the age of the oldest subgroups in Scorpius-Centaurus (~17 Myr), the simulations show 24 μm flux densities only 2–3 times photospheric as compared to the much larger ratios observed by Chen et al. (2005) and shown in Figure 7. This difference is independent of possible contamination by remnant primordial (or transition) disks in the Scorpius-Centaurus sample. In addition, there are no large excess ratios (spikes) greater than 2 after 50 Myr in the simulation results, unlike those of 2M 0735−1450 and HIP 8920 shown in Figure 7. Lastly, at no time before a hundred million years in the simulation does the 24 μm excess ratio reach unity. Any theory of debris disk evolution will have to account for those stars that show no 24 μm excess (within *Spitzer's* detection limits) at ages less than 100 Myr. This is an important observed phenomenon discussed earlier that occurs in stars across a broad range of spectral types and ages. Why some stars, in particular the youngest ($\lesssim$30 Myr), have mid-infrared excesses and others do not is still without clear explanation.

Additional mid-infrared observations of intermediate-mass stars with known ages should help further constrain the timescales and behavior of the evolution of debris disks and, ultimately, of planetary system formation.

5. CONCLUSIONS

We have conducted a photometric survey for dusty debris disks in the ~50 Myr open cluster IC 2391 with the MIPS 24 μm channel on *Spitzer*. This wavelength probes regions ~5–30 AU around A-type stars and regions ~1–5 AU around FGK stars. Due to the cluster's proximity, fluxes of stars as late as spectral type ~K4 can be measured down to the photospheric level. Of the 34 cluster members detected, only 10^{+17}_{-3}% (1/10) of the A-type stars had 24 μm flux densities $\geq$15% that of the photosphere. This is lower than the 31^{+13}_{-9}% (5/16) frequency measured for FGK stars in the cluster as well as marginally lower than A-type stars located in other young clusters. However, it is possible that this difference simply reflects random statistical variations.

In comparison, 31^{+13}_{-9}% of the FGK stars in IC 2391 have excesses. From their behavior, we find the following:

1. A high level of planetesimal activity (collisions) is still occurring in terrestrial planet regions (~1–5 AU) at ~50 Myr.
2. The fraction of FGK stars with 24 μm excesses decreases significantly on timescales of ~100 Myr. This decay over time corresponds to the observed decline of the frequency of collisions within the inner parts of these systems analogous to the asteroid belt of our own solar system.
3. The decay and variation of 24 μm excess ratios around FGK stars is very similar to that measured around A-type stars. Despite an overall decaying excess ratio evolution, there are large fractions of young stars with no excess at the youngest ages and rare large excesses at older ages indicative of episodic and stochastic events.
4. Despite differences in luminosity and in the annuli probed at 24 μm between A-type and FGK stars, debris disk evolution does not appear to be strongly influenced by stellar mass (for this range of spectral type).

N. S. would like to thank Christine Chen, Scott Kenyon, and Mike Meyer for helpful discussions and John Stansberry, Brian Patten, John Stauffer, and David Barrados y Navasqués for data pertaining to cluster membership. Support for this work was provided by NASA through contract 1255094 issued by JPL/Caltech. This research has made use of the SIMBAD and Vizier databases operated at CDS in Strasbourg, France; the Two Micron All Sky Survey (2MASS) data services, a joint project of the University of Massachusetts and the Infrared Processing Center/California Institute of Technology, funded by NASA and the NSF; and the US Naval Observatory (USNO) Naval Observatory Merged Astrometric Dataset (NOMAD). IRAF is distributed by the National Optical Astronomy Observatory, which is operated by the Association of Universities for Research in Astronomy, Inc., under contract to the NSF. E. E. M. is supported by a Clay Postdoctoral Fellowship from the Smithsonian Astrophysical Observatory.

APPENDIX A

LITERATURE SOURCES INCONSISTENT WITH CLUSTER MEMBERSHIP

The following sources are classified in the literature as possible or probable cluster members, but we conclude from this investigation that their properties are inconsistent with membership.

VXR PSPC 31.—Source at $08^h41^m11.0^s$, $-52^\circ31'46.0''$ is 0.47 mag below IC 2391 single-star sequence in Figure 2. In addition, both the Tycho-2 and UCAC2 proper motions exclude it as a member with high significance ($\chi^2/\nu \simeq 42/2$). In addition, colors and spectral type indicate evidence of reddening that is inconsistent with the overall cluster reddening. Despite evidence of youth (Randich et al. 2001), the source is likely to be a young background object rather than a cluster member.

HD 74517.—Tycho-2 proper motion is well-constrained but largely inconsistent with the Robichon et al. (1999) cluster mean ($\chi^2/\nu \simeq 320/2$). The nearly zero proper motion suggests that the source is likely to be an interloping A star rather than a cluster member.

HD 74665.—The proper motion is known to high accuracy, and the *Hipparcos*, Tycho-2, and UCAC2 proper motions exclude the star as a kinematic member ($\chi^2\nu \simeq 115/2$, 81/2, and 107/2, respectively). Source is likely an interloping A star rather than a cluster member.

APPENDIX B

COMMENTS ON INDIVIDUAL CLUSTERS

Scorpius-Centaurus OB association (16–17 Myr, 132 $\pm$ 14 pc).—Chen et al. (2005) have described a survey for excesses in this association's two oldest subgroups, Upper Centaurus Lupus ($\sim$17 Myr) and Lower Centaurus Crux ($\sim$16 Myr). Initial results show a 24 μm excess frequency of $\sim$40% (14/35 using a relative excess threshold $\geq$1.15; C. Chen 2007, private communication). Chen et al. (2005) state that the frequency could potentially be 40% higher if presumed interlopers are identified and removed from their proper-motion-selected sample. The large reported upper error bar in Table 5 is due to basing the uncertainty on this possible contamination. Age estimates are from Mamajek et al. (2005); distance is reported as typical stellar distances from the three subgroups (Chen et al. 2005).

Regarding the A-type stars in Upper Centaurus Lupus observed at 24 μm with *Spitzer* by Su et al. (2006), we used a 15% threshold in determining the number of excess sources so as to be consistent in our treatment of all the surveys. Su et al. (2006), however, with improved photometry and Kurucz photospheric model fitting, have reduced the threshold to 6% for the *Spitzer* A-type stars in their sample. Consequently, they measure an excess frequency of 56% (9/16), rather than the 44% (7/16) we report in Table 4 and shown in Figure 5.

NGC 2547 (30 $\pm$ 5 Myr, 450 $\pm$ 45 pc).—Using the Pleiades photospheric locus as the relative excess threshold and a larger list of cluster members, N. Gorlova et al. (2007, in preparation) have improved on the number of sources with 24 μm detections from Young et al. (2004) to now include F stars.

M47 (80 $\pm$ 20 Myr, 450 $\pm$ 50 pc).—The scatter of the $K_s - [24]$ color for FGK stars is relatively large with some sources appearing blueward of the Pleiades photospheric locus. While there were both F and G stars detected in the 24 μm investigation of M47 (Gorlova et al. 2004), the photometry was obtained during the *Spitzer* early checkout period during telescope commissioning, and data analysis techniques were still being optimized. Consequently, identifying excess sources among the FGK stars with a 15% threshold cannot yet be done with great confidence, and hence we do not use the cluster in our evolution analysis of FGK disk frequencies.

While we do not utilize the photometry of the solar-like stars in determining a debris disk frequency, we include M47 data in the excess ratio evolution (Fig. 7) since we are interested in the range of excesses rather than the frequency.

Hyades (625 $\pm$ 50 Myr, 46.3 $\pm$ 0.3 pc).—We include unpublished preliminary MIPS 24 μm results of the 625 Myr Hyades open cluster from a conference poster by Cieza et al. (2005), who report *no* sources with excess ratios clearly above $\sim$25%. At the 15% level, there is evidence for one borderline excess source from a rereduction of the public Hyades 24 μm data during this investigation. Age estimate is from Perryman et al. (1998).

Pleiades (115 $\pm$ 20 Myr, 135 $\pm$ 3 pc).—Fifty-three members of the Pleiades with spectral types between B8 and K6 have been analyzed by Stauffer et al. (2005) and Gorlova et al. (2006), identifying five with evidence of debris disks. References for cluster age and distance are taken from those within Gorlova et al. (2006).

Field stars.—Targeting 69 older, nearby field solar-type stars with median age $\sim$4 Gyr, Bryden et al. (2006) only found two objects with 24 μm excess $\geq$15% above the photosphere.

REFERENCES

Adams, F. C., Proszkow, E. M., Fatuzzo, M, & Myers, P. C. 2006, ApJ, 641, 504

Backman, D. E., & Paresce, F. 1993, in Protostars and Planets III, ed. E. H. Levy & J. I. Lunine (Tucson: Univ. Arizona Press), 1253

Backman, D. E., Stauffer, J. R., & Witteborn, F. C. 1991, in Bioastronomy: The Search for Extraterrestrial Life: The Exploration Broadens, ed. J. Heidmann & M. J. Klein (Berlin: Springer), 62

Baraffe, I., Chabrier, G., Allard, F., & Hauschildt, P. H. 1998, A&A, 337, 403

Barrado y Navascués, D., Stauffer, J. R., Briceño, C., Patten, B., Hambly, N. C., & Adams, J. D. 2001, ApJS, 134, 103

Barrado y Navascués, D., Stauffer, J. R., & Jayawardhana, R. 2004, ApJ, 614, 386

Beichman, C., et al. 2005a, ApJ, 622, 1160

———. 2005b, ApJ, 626, 1061

———. 2006, ApJ, 639, 1166

Bevington, P. R., & Robinson, D. K. 1992, Data Reduction and Error Analysis for the Physical Sciences (2nd ed.; New York: McGraw-Hill)

Binney, J., & Tremaine, S. 1987, Galactic Dynamics (Princeton: Princeton Univ. Press)

Bryden, G., et al. 2006, ApJ, 636, 1098

Burgasser, A. J., Kirkpatrick, J. D., Reid, I. N., Brown, M. E., Miskey, C. L., & Gizis, J. E. 2003, ApJ, 586, 512

Cambrésy, L., Beichman, C. A., Jarrett, T. H., & Cutri, R. M. 2002, AJ, 123, 2559

Carpenter, J. M. 2001, AJ, 121, 2851
Chambers, J. E. 2001, Icarus, 152, 205
Chen, C., Jura, M., Gordon, K. D., & Blaylock, M. 2005, ApJ, 623, 493
Chen, C. H., et al. 2006, ApJS, 166, 351
Chokshi, A., & Cohen, M. 1987, AJ, 94, 123
Cieza, L. A., Cochran, W. D., & Paulson, D. B. 2005, poster from Protostars and Planets V (Houston: LPI), http://www.lpi.usra.edu/meetings/ppv2005/pdf/8421.pdf
Cutri, R. M., et al. 2003, 2MASS All-Sky Catalog of Point Sources (Pasadena: IPAC)
Decin, G., Dominik, C., Waters, L. B. F. M., & Waelkens, C. 2003, ApJ, 598, 636
Dominik, C., & Decin, G. 2003, ApJ, 598, 626
Elmegreen, B. G. 2004, MNRAS, 354, 367
Forbes, M. C., Dodd, R. J., & Sullivan, D. J. 2001, Baltic Astron., 10, 375
Gautier, N., et al. 2006, ApJ, submitted
Gomes, R., Levison, H. F., Tsiganis, K., & Morbidelli, A. 2005, Nature, 435, 466
Gordon, K., et al. 2005, PASP, 117, 503
Gorlova, N., Rieke, G., Muzerolle, N., Stauffer, J., Siegler, N., Young, E. T., & Stansberry, J. H. 2006, ApJ, 649, 1028
Gorlova, N., et al. 2004, ApJS, 154, 448
Greaves, J. S., Fischer, D. A., & Wyatt, M. C. 2006, MNRAS, 366, 283
Habing, H. J., et al. 2001, A&A, 365, 545
Haisch, K. E., Lada, E. A., & Lada, C. J. 2001, ApJ, 553, L153
Hines, D., et al. 2006, ApJ, 638, 1070
Hollenbach, D. J., Yorke, H. W., & Johnstone, D. 2000, in Protostars and Planets IV, ed. V. Mannings, A. P. Boss, & S. S. Russell (Tucson: Univ. Arizona Press), 401
Jacobsen, S. B. 2005, Annu. Rev. Earth Planet. Sci., 33, 531
Johnstone, E., Hollenback, D., & Bally, J. 1998, ApJ, 499, 758
Kenyon, S. J., & Bromley, B. C. 2004a, ApJ, 602, L133
———. 2004b, AJ, 127, 513
———. 2005, AJ, 130, 269
Kim, J. S., et al. 2005, ApJ, 632, 659
Kleine, T., Munker, C., Mezger, K., & Palme, H. 2002, Nature, 418, 952
Lagrange, A.-M., Backman, D. E., & Artymowicz, P. 2000, in Protostars and Planets IV, ed. V. Mannings, A. P. Boss, & S. S. Russell (Tucson: Univ. Arizona Press), 639
Liu, M. C., Matthews, B. C., Williams, J. P., & Kalas, P. G. 2004, ApJ, 608, 526
Mamajek, E. E., et al. 2005, ApJ, 634, 1385
Marino, A., Micela, G., Peres, G., Pillitteri, I., & Sciortino, S. 2005, A&A, 430, 287
Matsuyama, I., Johnstone, G., & Murray, N. 2003, ApJ, 585, L143
Meyer, M. R., et al. 2004, ApJS, 154, 422
Monet, D. G., et al. 2003, AJ, 125, 984
Nissen, P. E. 1988, A&A, 199, 146
Papovich, C., et al. 2004, ApJS, 154, 70
Patten, B. M., & Pavlovsky, C. M. 1999, PASP, 111, 210
Patten, B. M., & Simon, T. 1993, ApJ, 415, L123
———. 1996, ApJS, 106, 489
Perryman, M. A. C., et al. 1998, A&A, 331, 81
Randich, S., Pallavicini, R., Meola, G., Stauffer, J. R., & Balachandran, S. C. 2001, A&A, 372, 862
Richling, S., & Yorke, H. W. 1998, A&A, 340, 508
Rieke, G., et al. 2004, ApJS, 154, 25
———. 2005, ApJ, 620, 1010
Robichon, N., Arenou, F., Mermilliod, J.-C., & Turon, C. 1999, A&A, 345, 471
Sagar, R., & Bhatt, H. C. 1989, MNRAS, 236, 865
Siess, L., Dufour, E., & Forestini, M. 2000, A&A, 358, 593
Silverstone, M., et al. 2006, ApJ, 639, 1138
Simon, T., & Patten, B. M. 1998, PASP, 110, 283
Song, I., Weinberger, A. J., Becklin, E. E., Zuckerman, B., & Chen, C. 2002, AJ, 124, 514
Song, I., Zuckerman, B., Weinberger, A. J., & Becklin, E. E. 2005, Nature, 436, 363
Spangler, C., Sargent, A. I., Silverstone, M. D., Becklin, E. E., & Zuckerman, B. 2001, ApJ, 555, 932
Stauffer, J., Hartmann, L. W., Jones, B. F., & McNamara, B. R. 1989, ApJ, 342, 285
Stauffer, J., et al. 1997, ApJ, 479, 776
———. 2005, AJ, 130, 1834
Strom, R. G., Malhotra, R., Ito, T., Yoshida, F., & Kring, D. 2005, Science, 309, 1847
Su, K. Y. L., et al. 2006, ApJ, submitted
Throop, H. B., & Bally, J. 2005, ApJ, 623, L149
Wyatt, M. C. 2005, A&A, 433, 1007
Young, E., et al. 2004, ApJS, 154, 428
Zacharias, N., Monet, D. G., Levine, S. E., Urban, S. E., Gaume, R., & Wycoff, G. L. 2004a, BAAS, 36, 1418
Zacharias, N., et al. 2004b, AJ, 127, 3043
Zuckerman, B. 2001, ARA&A, 39, 549